J Mater Sci (2008) 43:2680–2685
DOI 10.1007/s10853-007-2439-3

Geometrical analysis of near polyhedral shapes with round edges in small crystalline particles or precipitates

Susumu Onaka

Received: 17 July 2007 / Accepted: 28 December 2007 / Published online: 19 February 2008

Abstract Small crystalline particles or precipitates are often formed comprising near polyhedral shapes with round edges. Using the anisotropy of the surface energy given by a simple broken-bond model for fcc crystals, a geometrical analysis is performed to consider the particle-shape dependence of surface energy. Polyhedral and nearly polyhedral particles composed of {100} and {111} planes are treated as examples. The effect of round edges on the variation of surface energy of the nearly polyhedral particles is discussed.

Introduction

Various factors affect the shapes of small metals particles or precipitates in alloys. The crystal structure represents one of the factors, since the shapes of the particles or precipitates sometimes show symmetry reflecting the symmetry of the alloy crystal structure. Indeed, polyhedral shapes composed of low-index planes are typical examples of such symmetrical shapes [1–6]. For materials having cubic crystal structures, the small particles or precipitates often show shapes similar to polyhedra composed of the low-index planes, {100}, {110}, and {111} [1–6]. However, the shapes are in general not perfect polyhedra but are instead nearly polyhedral with rounded edges [1–6].

To discuss the origins of the shapes of the small particles or precipitates in a physically sound manner, simple equations describing the shapes are effective [1, 7–9]. Recently, Onaka derived simple equations to describe various polyhedra and similar shapes intermediate between those of a polyhedron and a sphere [10, 11]. A parameter giving the degree of polyhedrality of the intermediate shape is given by equations in the literature [1, 9]. Using these equations [1, 9–11], we consider geometrically the effect of the round edges of the near polyhedral shapes on the variation of the surface energy of crystalline particles. In the present paper, the anisotropy of surface energy given by a simple broken-bond model for face-centered cubic (fcc) crystals [12] is assumed as a simplified state. The polyhedra composed of the following two kinds of low-index planes, {100} and {111}, and the corresponding intermediate shapes somewhere between such polyhedra and a sphere are discussed.

Simple equations yielding polyhedra, spheres, and intermediate shapes

The following equation using the x–y–z orthogonal coordinate system gives the shapes of a sphere, a cube, and intermediate shapes by choosing an appropriate value of p [1, 9–11, 13]:

$$|x/R|^p + |y/R|^p + |z/R|^p = 1 (R > 0, p \geq 2). \quad (1)$$

A sphere with radius R is given by Eq. 1 when $p = 2$, and a cube with edges $2R$ is given by Eq. 1 when $p \to \infty$. Figure 1 shows the shapes given by Eq. 1 with intermediate values of p: (a) the $x-y$ cross sections for $p = 2$, $p = 4$, and $p = 20$, and (b) the 3D representation for $p = 20$. The shapes given by Eq. 1 with round edges have been discussed as representative of the approximate shapes of Co–Cr precipitates in Cu alloys [1].

S. Onaka (✉)
Department of Materials Science and Engineering,
Tokyo Institute of Technology, 4259 Nagatsuta,
Yokohama 226-8502, Japan
e-mail: onaka@iem.titech.ac.jp

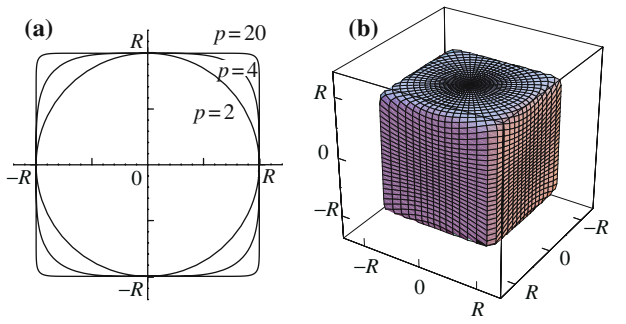

Fig. 1 The shapes given by Eq. 1 with intermediate values of p: (**a**) the $x-y$ cross sections for $p = 2$, $p = 4$, and $p = 20$, and (**b**) the 3D representation for $p = 20$

Using the spherical coordinates (r, θ, φ), Eq. 1 is rewritten as [10]:

$$r_{\text{cube}}(\theta,\varphi) = \frac{R}{[G_0(1,0,0)]^{1/p}}, \tag{2a}$$

where

$$G_0(1,0,0) = |g(1,0,0)|^p + |g(0,1,0)|^p + |g(0,0,1)|^p \tag{2b}$$

and

$$g(a,b,c) = a(\sin\theta\cos\varphi) + b(\sin\theta\sin\varphi) + c(\cos\theta). \tag{2c}$$

In the present paper, we discuss the polyhedral and nearly polyhedral shapes of materials with cubic structures. Then, assuming that the x, y, and z axes are parallel to the $\langle 100\rangle$ directions of the cubic materials, the surfaces of the cube become the $\{100\}$ planes.

Onaka has shown that the shapes of various convex polyhedra and intermediate shapes somewhere between the polyhedra and a sphere are given by equations similar to Eqs. 2a–2c [10]. Four sets of parallel $\{111\}$ surfaces of cubic materials combine to form an octahedron. A unit vector normal to the (111) plane is (γ, γ, γ) and $\gamma = 1/\sqrt{3}$. Then, an octahedron and intermediate shapes somewhere between the octahedron and a sphere are given by:

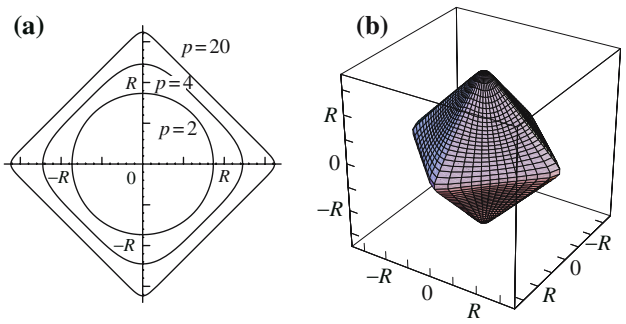

Fig. 2 The shapes given by Eqs. 3a and 3b with intermediate values of p: (**a**) the $x-y$ cross sections for $p = 2$, $p = 4$, and $p = 20$, and (**b**) the 3D representation for $p = 20$

$$r_{\text{octa}}(\theta,\varphi) = \frac{R}{[G_{\text{I}}(\gamma,\gamma,\gamma)]^{1/p}}, \tag{3a}$$

where

$$G_{\text{I}}(\gamma,\gamma,\gamma) = |g(\gamma,\gamma,\gamma)|^p + |g(-\gamma,\gamma,\gamma)|^p + |g(\gamma,-\gamma,\gamma)|^p + |g(\gamma,\gamma,-\gamma)|^p. \tag{3b}$$

Figure 2 shows the shapes given by Eqs. 3a and 3b: (a) the $x-y$ cross sections for $p = 2$, $p = 4$, and $p = 20$, and (b) the 3D representation for $p = 20$. As is the case for Eq. 1, and Eqs. 2a and 2b, Eqs. 3a and 3b generate a sphere and a polyhedron when $p = 2$ and $p \to \infty$, respectively.

Here, we consider the following equation given by the combination of G_0 (1,0,0) for the cube and G_{I} (γ,γ ,γ) for the octahedron:

$$r(\theta,\varphi) = \frac{R}{\left[G_0(1,0,0) + \left(\sqrt{3}\alpha\right)^p G_{\text{I}}(\gamma,\gamma,\gamma)\right]^{1/p}}, \tag{4}$$

where α is the parameter that determines the relative importance of G_{I} (γ,γ,γ) compared with G_0 (1,0,0). Figure 3 shows the shapes given by Eq. 4 with $\alpha = 1/\sqrt{3}$: (a) the $x-y$ cross sections for $p = 2$, $p = 10$, and $p = 40$, and (b–d) the 3D representation for these values of p. Equation (4) gives a sphere when $p = 2$ for any $\alpha \geq 0$.

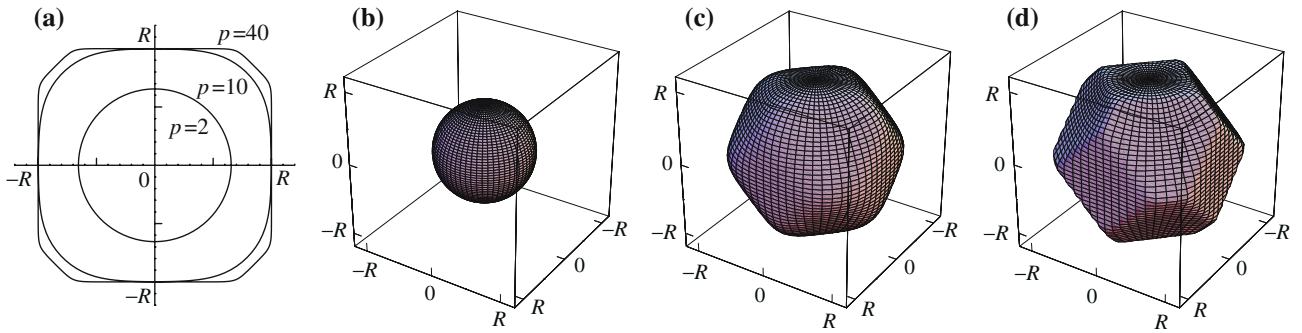

Fig. 3 The shapes given by Eq. 4 with $\alpha = 1/\sqrt{3}$: (**a**) the $x-y$ cross sections for $p = 2$, $p = 10$, and $p = 40$, and (**b–d**) the 3D representations for these values of p

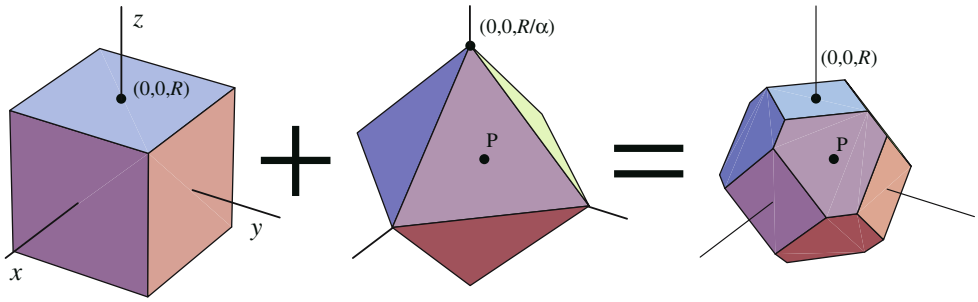

Fig. 4 The polyhedron afforded by the addition of the {100} cube and the {111} octahedron, which is given by Eq. 4 with $p \to \infty$

Equation 4 gives shapes approaching polyhedra composed of {100} and {111} planes with increasing p. The shape of the polyhedron given by $p \to \infty$ is a function of α. When $p \to \infty$, Eq. 4 gives the {100} cube for the range $0 \le \alpha \le 1/3$ and the {111} octahedron for the range $1 \le \alpha$. The shape change of the polyhedron from the {100} cube to the {111} octahedron occurs as a result of truncation when the value of α is increased from 1/3 to 1 [10, 11]. As shown in Fig. 4, Eq. 4 with $p \to \infty$ gives a polyhedron made by the combination of the {100} cube and the {111} octahedron. The {100} cube with constant edges $2R$ is truncated by the {111} octahedron having a vertex with the position of $(0, 0, R/\alpha)$. The size of the {111} octahedron is proportional to $1/\alpha$. The point P on the {111} octahedron and its position on the combined polyhedron are shown in Fig. 4. The α dependence of the shape of the combined polyhedron given by Eq. 4 is thus understood.

Figure 5 shows the variation of $A/V^{2/3}$ as a function α given by Eq. 4 with $p \to \infty$, where A and V are the surface area and volume of the polyhedron, respectively. The dimensionless value $A/V^{2/3}$ is the normalized surface area of the polyhedron when V is kept constant. The insets in Fig. 5 show the shapes of the {100}−{111} polyhedra for various α. For the {100}−{111} polyhedra, $A/V^{2/3}$

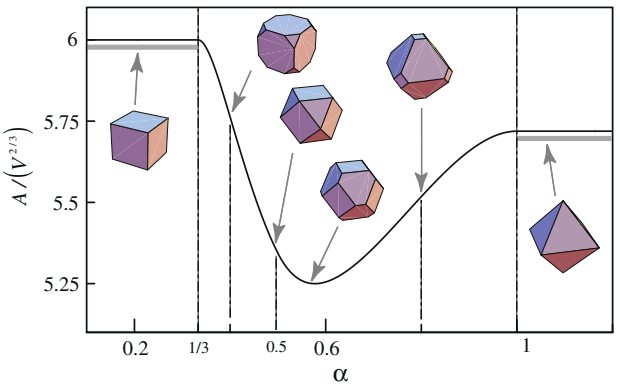

Fig. 5 The variation of $A/V^{2/3}$ as a function of the parameter α caused by the shape change of polyhedron given by Eq. 4 with $p \to \infty$, where A and V are the surface area and volume of the polyhedron, respectively. The insets show the variation of shapes of the {100}−{111} polyhedra as a function of α

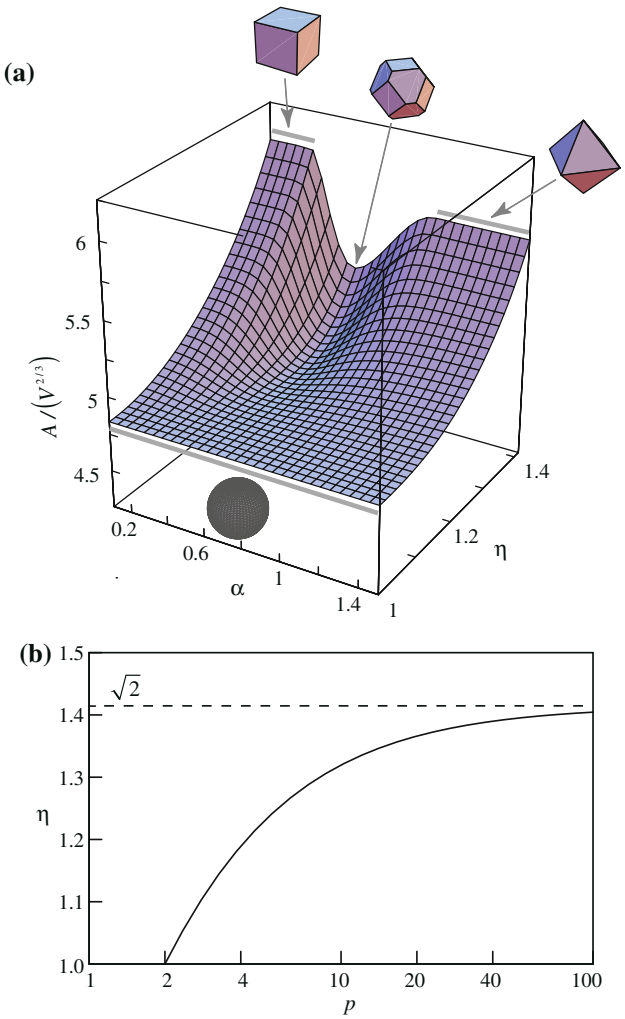

Fig. 6 The geometrical variation caused by the shape changes from a sphere to various {100}−{111} polyhedra given by Eq. 4. (**a**) The 3D representation showing the variation of $A/V^{2/3}$ as a function of α and η, and (**b**) the relationship between p and η given by Eq. 5. The insets in (**a**) are the shapes at the indicated values of α and η

becomes a minimum when $\alpha = 1/\sqrt{3}$. Explicit expressions of the surface area A and volume V of the {100}−{111} polyhedra are shown in the Appendix.

Figure 6a shows the variation of $A/V^{2/3}$ caused by the shape changes from a sphere to various {100}−{111}

polyhedra given by Eq. 4. The insets showing the shapes are also indicated in Fig. 6a. In this 3D representation, one of the axes shows the change in η, where η is the degree of polyhedrality given by:

$$\eta = \sqrt{2} \cdot 2^{(-1/p)}. \tag{5}$$

The parameter η equals unity when $p = 2$(sphere) and $\sqrt{2}$ when $p \to \infty$ and the particle is fully faceted. The relationship between p and η is shown graphically in Fig. 6b.

Kimoto and Nishida have studied the morphology of Al particles made by evaporation in a clean atmosphere of argon [2]. When the Al particles are isolated, they have the near {100}−{111} polyhedral shape with round edges as shown by Figs. 2a and 3a in their paper [2]. In the case of the Al particle with diameter about 150 nm [2], the shape is evaluated by the present method of analysis as $\alpha \approx 0.61$ and $p \approx 15$ ($\eta \approx 1.35$).

Anisotropic surface-energy density given by a simple model

If the surface-energy density is isotropic, the variation of $A/V^{2/3}$ shown in Fig. 6a represents the particle-shape dependence of the surface energy under a constant volume. However, the surface-energy density of crystalline materials is essentially anisotropic and, of course, this is an important factor when we discuss the shape of the particles or precipitates.

The formation of surfaces in crystalline materials invariably results in the breaking of interatomic bonds across the surfaces. A theoretical explanation for the anisotropy of the surface-energy density has been made by considering the difference in the bonds broken as a result of the difference in the orientation of surface. The simplest treatment may be that of Mackenzie et al. which is more commonly known as the nearest-neighbor broken-bond model [12]. For face-centered cubic crystals, the result obtained by Mackenzie et al. [12] is written as:

$$\gamma_h = (v_h \cdot v_{210})\gamma_{210}, \tag{6}$$

where γ_h is the surface-energy density for the surface with the unit normal vector v_h, γ_{210} is the maximum surface-energy density for the {210} plane, and v_{210} is the unit normal vector of the {210} plane. To calculate the value of γ_h, the unit vector v_{210} should be selected so that it is on the edge of the stereographic triangle that contains v_h. The contours of γ_h/γ_{210} and the values for {100}, {110}, and {111} are shown in Fig. 7. As shown in Fig. 7, γ_h for {111}, γ_{111} is the lowest, while γ_{100} is less than γ_{110}. The ratio $\gamma_{\{111\}}/\gamma_{\{100\}}$ given by Eq. 6 is $\sqrt{3}/2$.

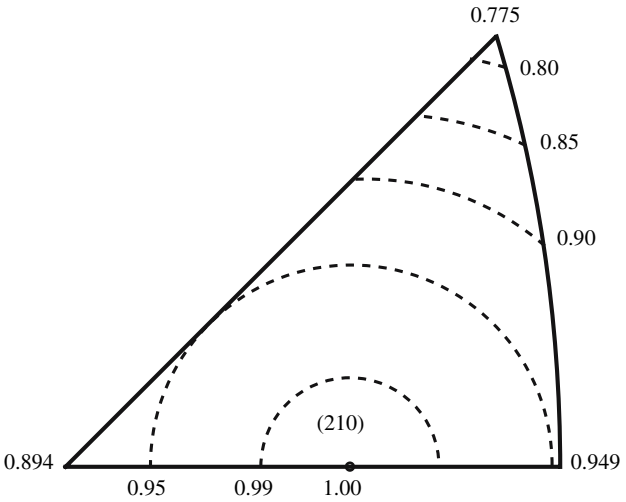

Fig. 7 Surface-energy contours showing the values of γ_h/γ_{210} given by Eq. 6 based on the broken-bond model for face-centered cubic crystals [12]

Surface energy of polyhedral and nearly polyhedral particles

Using the surface-energy density γ_h, the total surface energy Γ of a particle is written as:

$$\Gamma = \sum \gamma_h ds, \tag{7}$$

where ds is the surface element on the particle and the summation of $\gamma_h ds$ is made on the entire surface. When the volume of the particle is V, the dimensionless value

$$N_\Gamma = \Gamma / \left(\gamma_{210} V^{2/3}\right) = \sum \gamma_h ds / \left(\gamma_{210} V^{2/3}\right) \tag{8}$$

shows the particle-shape dependence of the surface energy.

For the particles whose shapes are given by Eqs. 4 and 5, the α and η dependence of $N_\Gamma = \sum \gamma_h ds / \left(\gamma_{210} V^{2/3}\right)$ is shown by the 3D representation in Fig. 8a. Some shapes of the particles are indicated by the insets in this figure. The shape of the particle giving the minimum $N_\Gamma \approx 4.26$ is the polyhedron with $\alpha = 2/3$, which is the equilibrium shape when the anisotropy of the surface energy is given by Eq. 6. That is to say, this is the shape given by the so-called Wulff plot. The polyhedron with $\alpha = 2/3$ is known as a tetrakaidecahedron having eight regular hexagonal surfaces and six square surfaces.

We have also considered the variation of N_Γ as a function of the degree of polyhedrality η when α is determined so that α minimizes $N_\Gamma(\alpha)$. Figure 8b shows the results, i.e., the variation of the minimum of $N_\Gamma(\alpha)$ as a function of η. The insets of the particle shapes in this figure are for those of $\eta = 1$ ($p = 2$) for a sphere, $\eta \approx 1.30$ ($p \approx 8.23$), and $\eta \approx 1.38$ ($p \approx 28.3$) for nearly polyhedral shapes with round edges, and the equilibrium polyhedron

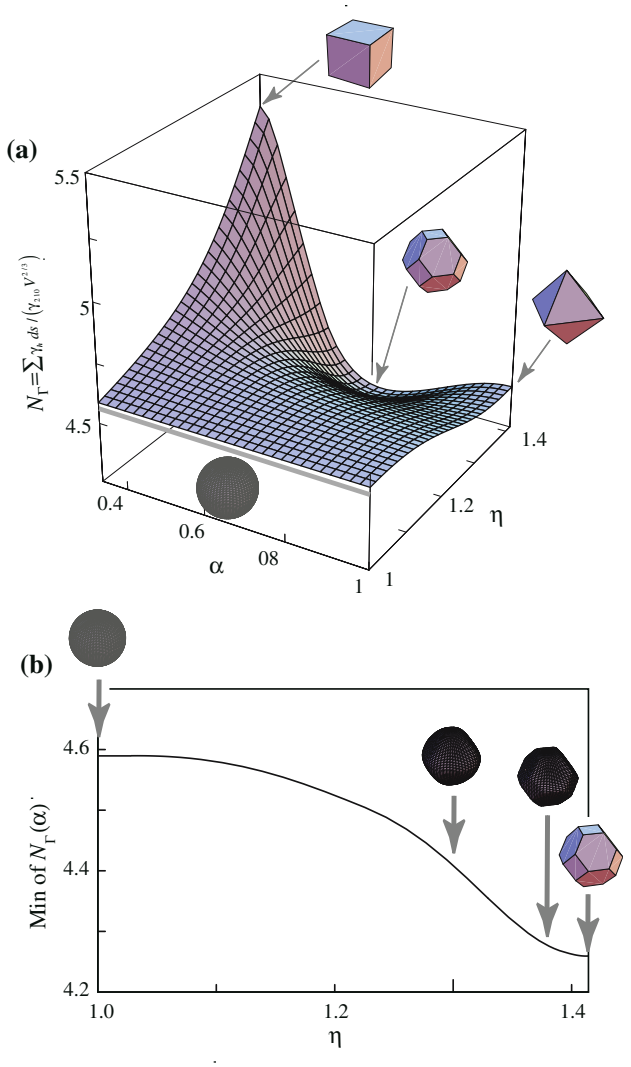

Fig. 8 The variation of the normalized surface energy $N_\Gamma = \sum \gamma_h ds/(\gamma_{210}V^{2/3})$ caused by the shape changes from a sphere to various $\{100\}-\{111\}$ polyhedra given by Eq. 4. (**a**) The 3D representation showing the variation of N_Γ as a function of α and η, and (**b**) the variation of the minimum of $N_\Gamma(\alpha)$ as a function of η. The insets in (**a**) and (**b**) are the shapes at the indicated values of α and/or η

with $\eta = \sqrt{2}$ $(p \to \infty.)$ Comparing this result with the p dependence of the shape change, we find that the round edges of the nearly polyhedral shapes do not increase the surface energy significantly. This means that the driving force to achieve the equilibrium state becomes smaller for the near polyhedral shapes with round edges.

The present analysis is made using the anisotropy of the surface energy given by the simple broken-bond model. However, the geometrical characteristics of the near polyhedral shapes with round edges are appropriately included in the evaluation of the surface energy. The same discussion can be made for near polyhedral shapes by using more rigorous results on the anisotropy of the surface energy. The effect of round edges on the interface energy between the precipitates and the matrix can also be evaluated by the present method. Near polyhedral particles or precipitates are often observed in many alloys [1–6]. If the equilibrium shape and the relative energies of the surface are known, we can evaluate the shape dependence of the surface or interface energy using the present method of analysis.

Acknowledgements The present work was supported by a Grant-in-Aid for Scientific Research from the Ministry of Education, Culture, Sports, Science and Technology of Japan.

Appendix

The surface area A and volume V of the $\{100\}-\{111\}$ polyhedra are given by Eq. 4 with $p \to \infty$.

For the $\{100\}-\{111\}$ polyhedra given by Eq. 4 with $p \to \infty$, the surface area $A = A_{100} + A_{111}$ and the volume V are given by as follows, where A_{100} and A_{111} correspond to the areas of the $\{100\}$ and $\{111\}$ surfaces, respectively. The variation of shapes of the $\{100\}-\{111\}$ polyhedra as a function of α is shown in the insets in Fig. 5.

(1) When $0 \le \alpha \le 1/3$, Eq. 4 gives the $\{100\}$ cube with edges $2R$:

$$A_{100} = 24R^2, \quad A_{111} = 0 \text{ and } V = 8R^3.$$

(2) When $1/3 \le \alpha \le 1/2$, Eq. 4 gives a polyhedron with triangular $\{111\}$ surfaces, which is inscribed in the cube with edges $2R$:

$$A_{100} = 24\left\{1 - \tfrac{1}{2}\left(3 - \tfrac{1}{\alpha}\right)^2\right\}R^2, \quad A_{111} = 4\sqrt{3}\left(3 - \tfrac{1}{\alpha}\right)^2 R^2$$
$$\text{and} \quad V = 8\left\{1 - \tfrac{1}{6}\left(3 - \tfrac{1}{\alpha}\right)^3\right\}R^3.$$

(3) When $1/2 \le \alpha \le 1$, Eq. 4 gives a polyhedron with square $\{100\}$ surfaces, which is inscribed in the cube with edges $2R$:

$$A_{100} = \tfrac{12}{\alpha^2}(1-\alpha)^2 R^2, \quad A_{111} = \tfrac{4\sqrt{3}}{\alpha^2}\left\{1 - 3(1-\alpha)^2\right\}R^2$$
$$\text{and} \quad V = \tfrac{4}{3\alpha^3}\left\{1 - 3(1-\alpha)^3\right\}R^3.$$

(4) When $1 \le \alpha$, Eq. 4 gives the $\{111\}$ octahedron with edges $\sqrt{2}R/\alpha$:

$$A_{100} = 0, \quad A_{111} = \tfrac{4\sqrt{3}}{\alpha^2}R^2 \text{ and } V = \tfrac{4}{3\alpha^3}R^3.$$

References

1. Onaka S, Kobayashi N, Fujii T, Kato M (2003) Mater Sci Eng A 347:42
2. Kimoto K, Nishida I (1977) Jpn J Appl Phys 16:941
3. Sundquist BE (1964) Acta Metall 12:67
4. Heyraud JC, Metois JJ (1980) Acta Metall 28:1789

5. Heyraud JC, Metois JJ (1983) Surf Sci 128:334
6. Furuhara T, Kimori T, Maki T (2006) Metall Mater Trans A37:951
7. Onaka S, Kobayashi N, Fujii T, Kato M (2002) Intermetallics 10:343
8. Onaka S (2005) Phil Mag Lett 85:359
9. Onaka S (2001) Phil Mag Lett 81:265
10. Onaka S (2006) Phil Mag Lett 86:175
11. Onaka S, Fujii T, Kato M (2007) Acta Mater 55:669
12. Mackenzie JK, Moore AJW, Nicholas JF (1962) J Phys Chem Solids 23:185
13. Jaklic A, Leonardis A, Solina F (2000) Segmentation and recovery of superquadrics (Computational imaging and vision, vol 20). Kluwer Academic, Norwell, p 13